

Supporting Information

Boosting photoreduction of CO₂ via Synergistic Cu-Ag Bimetallic Sites on Carbon Nitride

Jingru Wang, Jinke Li, Zhenbo Zhang, Hao Shi, Jiayi Wan, Yiming Zhou, Tong Bian* and Huijun Yu*

School of Chemistry and Chemical Engineering, Southeast University, Nanjing 211189, China.

Corresponding author: Prof. Tong Bian and Prof. Huijun Yu

E-mail: tbian@seu.edu.cn; yuhuijun@seu.edu.cn

Materials

In this study, all chemicals were used directly as purchased without further purification. Melamine, copper nitrate ($\text{Cu}(\text{NO}_3)_2 \cdot 3\text{H}_2\text{O}$), dimethyl sulfoxide (DMSO) and sodium sulfate anhydrous (Na_2SO_4) were sourced from Meryer Biochemical Technology company. Cyanuric acid and methanol were sourced from Shanghai Macklin Biochemical company. Ethanol and silver nitrate (AgNO_3) were sourced from Sinopharm Chemical Reagent Co.Ltd.. Deionized water was sourced from Nanjing Jingge Chemical Technology company. High purity CO_2 (99.999%) and pure N_2 (99.999%) were sourced from Nanjing Special Gas Company.

Materials Synthesis

Preparation of CN

0.51 g of cyanuric acid and 0.5 g of melamine were dissolved in 10 mL and 20 mL DMSO, respectively. After complete dissolution, both solutions were mixed together for 30 min to obtain a white precipitate. Then, the white precipitate was washed three times by centrifugation with ethanol (12000 r/min, 10 min), and then dried at 60 °C overnight. Finally, the resulting solid was calcined at 550 °C for 4 h with the heating rate of 4 °C/min.

Preparation of CuAg/CN

20 mg CN was added to 36 mL deionized water and 4 mL methanol sonicated form a suspension solution. Then, the solution was purged with N_2 for 30 min to remove the dissolved O_2 . $\text{Cu}(\text{NO}_3)_2 \cdot 3\text{H}_2\text{O}$ solution (2 mg/mL, 1 mL) was added into the above mixture and then illuminated under mercury lamp for 30 min with stirring. Subsequently, AgNO_3 solution (0.8 mg/mL, 1 mL) was also added into the above mixture and irradiated for another 30 min. The product was washed three times by centrifugation with deionized water (12000 r/min, 10min), and then dried at 60 °C overnight.

Preparation of Cu/CN, Ag/CN and AgCu/CN

The synthesis of Cu/CN and Ag/CN followed the similar procedure as that of CuAg/CN, except without silver source or copper source added.

The synthesis of AgCu/CN followed the similar procedure as that of CuAg/CN, except that the addition sequence of $\text{Cu}(\text{NO}_3)_2 \cdot 3\text{H}_2\text{O}$ and AgNO_3 is exchanged.

Preparation of AgCu-T/CN

20 mg CN was added to 36 mL deionized water and 4 mL methanol sonicated

form a suspension solution. Then, the solution was purged with N₂ for 30 min to remove the dissolved O₂. Cu(NO₃)₂·3H₂O solution (2 mg/mL, 1 mL) and AgNO₃ solution (0.8 mg/mL, 1 mL) were added into the above mixture at the same time and then illuminated under mercury lamp for 30 min with stirring. The product was washed three times by centrifugation with deionized water (12000 r/min, 10min), and then dried at 60 °C overnight.

Photocatalytic CO₂ reduction testing

In brief, 5 mg of the catalyst was dispersed in 2 mL of isopropanol suspension was prepared before testing. Then, 400 μL of the catalyst suspension was loaded onto a 2 cm*2 cm glass sheet and transferred to the reactor vessel. Subsequently, the reaction system was evacuated and purged with high-purity CO₂ (99.99%) three times to remove the air in the reactor. The photocatalytic CO₂ reduction was initiated under irradiation from a 300 W Xe lamp. The gas products were detected and analyzed by as Gas Chromatograph (GC-2014C, Shimadzu), which was equipped with TCD detector and FID detector (Ar as the carrier gas).

Characterizations

Scanning electron microscopy (SEM, Crossbeam350), TEM and High-resolution TEM images (Talos P200X G2) with an energy-dispersive X-ray spectrometer (EDS) were adopted to observed the morphologies of the samples. The X-ray diffraction (XRD) measurements were carried out on a powder X-ray diffractometer with a Cu-Kα radiation source, (Ultima IV, RIGAKU). A Nicolet iS10 Fourier transform instrument was used to record Fourier transform infrared (FTIR) spectrum. X-ray photoelectron spectroscopy (XPS) tests performed on a SCIENTIFIC K-ALPHA (Thermo) electron spectrometer, where C 1s at 284.8 eV was used as a reference. UV-Vis diffused reflection spectra were determined at room temperature on a spectrophotometer (UV-2600, Shimadzu). The specific surface area was analyzed using an automatic specific surface area and microporous physical adsorption instrument (BET, ASAP2460). Photoluminescence (PL) measurement was conducted on a fluorescence spectrometer (horiba france fluoromax-) at an excitation wavelength of 360 nm. In situ diffuse reflectance infrared Fourier transform spectra (DRIFTS) are acquired on a Thermo Fisher-Nicolet iS50 spectrometer.

Photoelectrochemical measurements

Photoelectrochemical tests were conducted on the electrochemical workstation (CHI760E) using a three-electrode system. The Pt electrode and the Ag/AgCl electrode are respectively used as the counter electrode and the reference electrode. A 300 W Xe lamp was used as the light source and 0.5 M Na₂SO₄ as the electrolyte. In detail, the working electrode was prepared by 1mg of the catalyst sample was dispersed in 5 mL of isopropanol (with 20 μL of Nafion solution added), and 50 μL of

the dispersion was loaded onto a 1 cm*1 cm FTO glass sheet.

Supplementary Figures

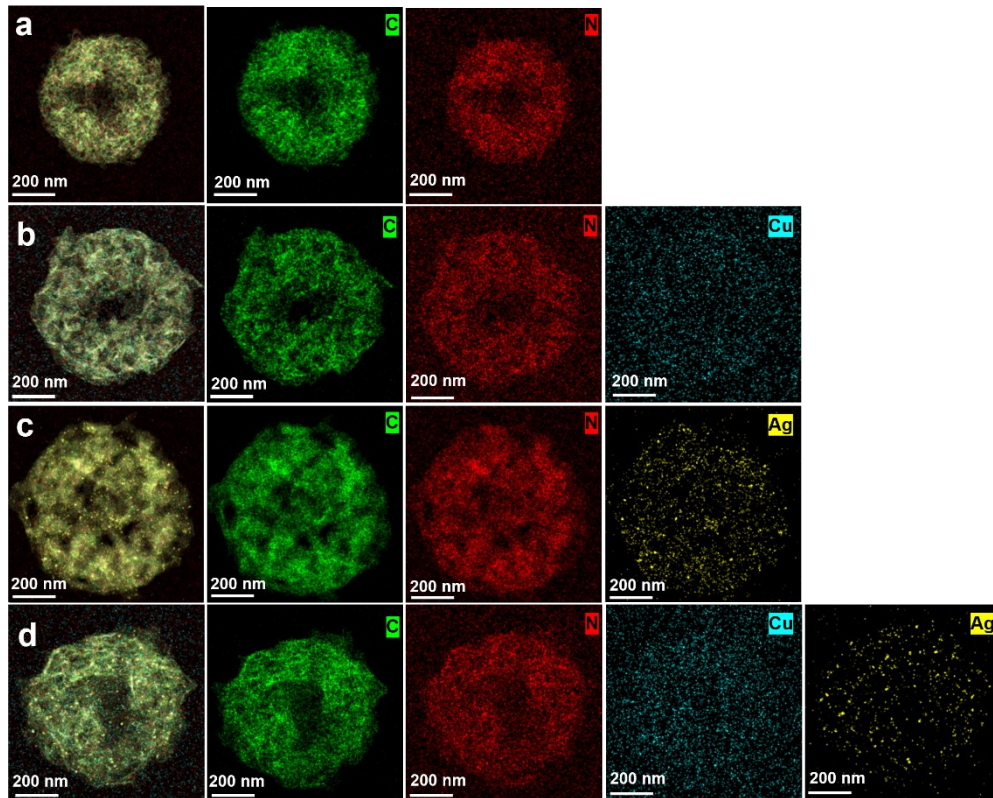


Fig.S1 EDS elemental mapping of (a) CN, (b) Cu/CN, (c) Ag/CN, (d) AgCu/CN, respectively.

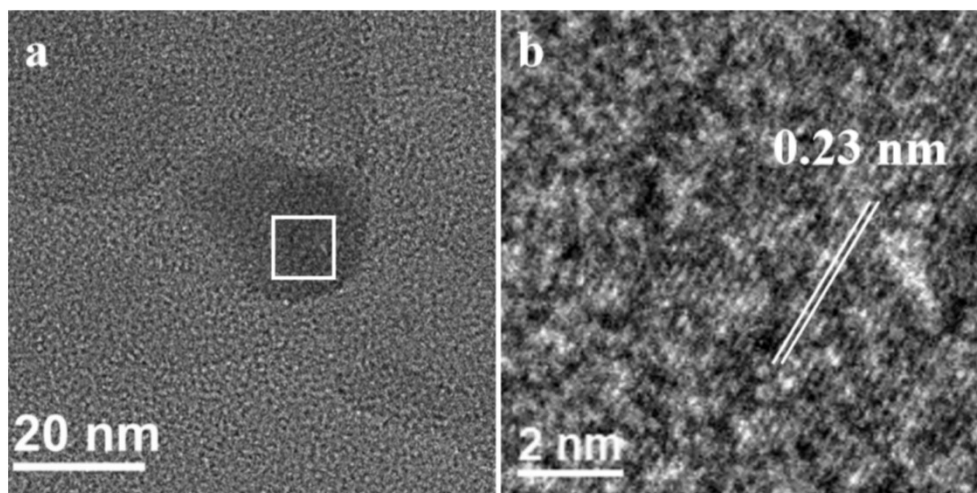


Fig.S2 HRTEM image of Ag/CN with the lattice fringe of 0.23 nm assigned to Ag⁰.

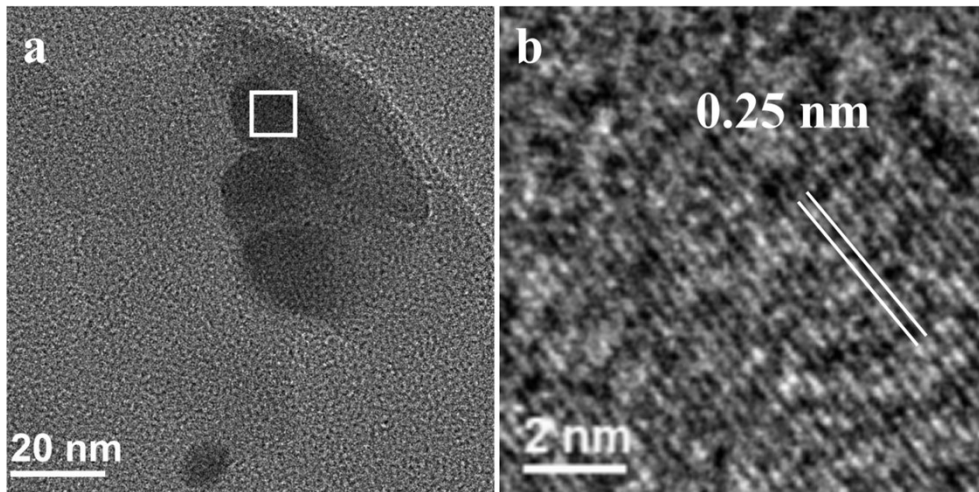


Fig.S3 HRTEM image of AgCu/CN with the lattice fringe of 0.25 nm assigned to Ag⁰.

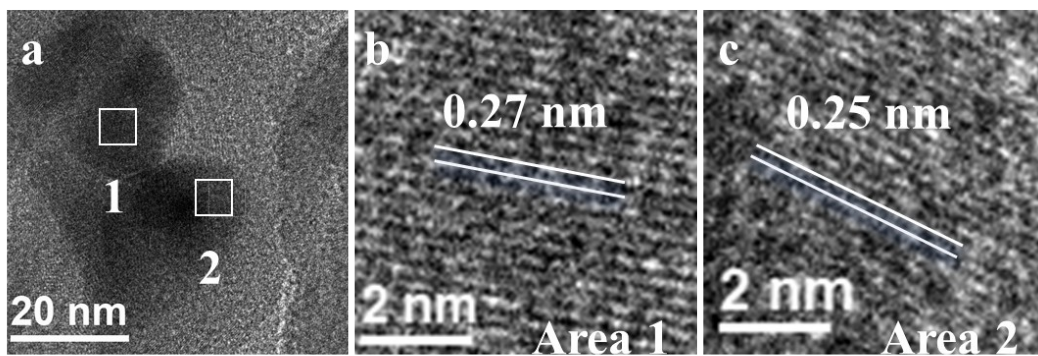


Fig.S4 HRTEM image of CuAg/CN with the lattice fringe of 0.25 and 0.27 nm assigned to Ag^0 and Ag_2O respectively.

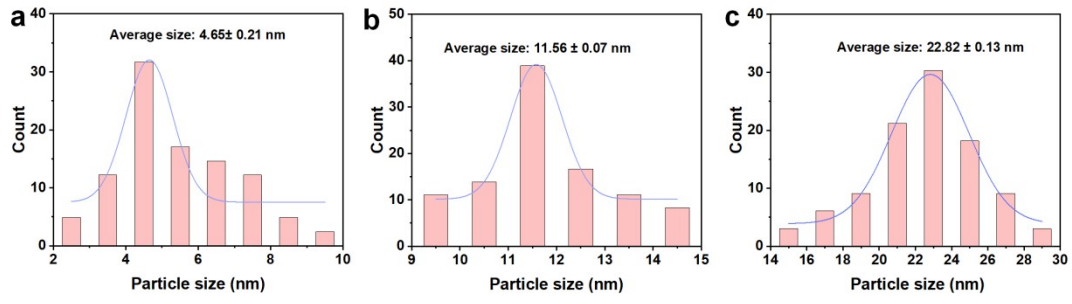


Fig.S5 Size distribution images of (a) Ag/CN, (b) AgCu/CN and (c) CuAg/CN.

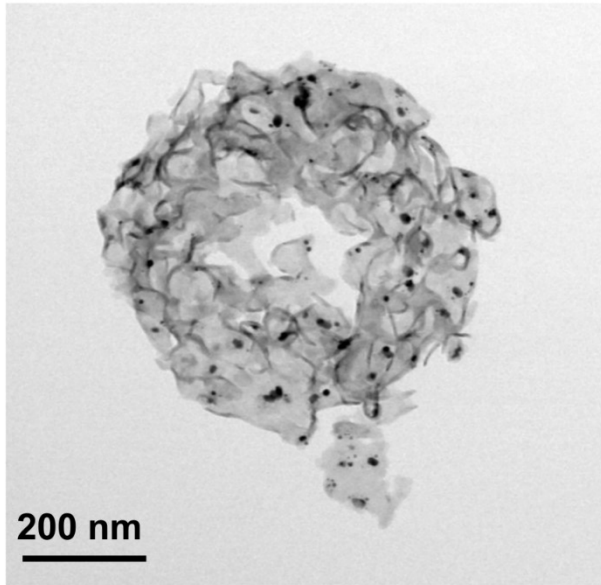


Fig.S6 TEM image of AgCu-T/CN.

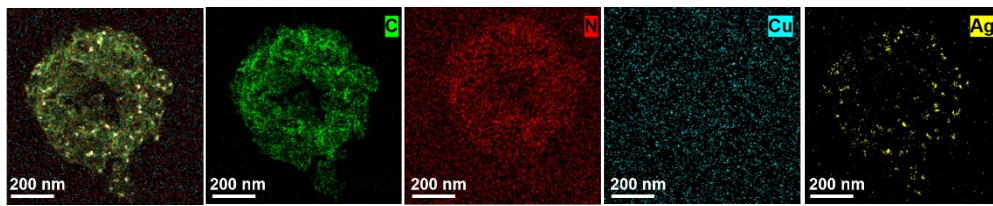


Fig.S7 EDS elemental mapping of AgCu-T/CN.

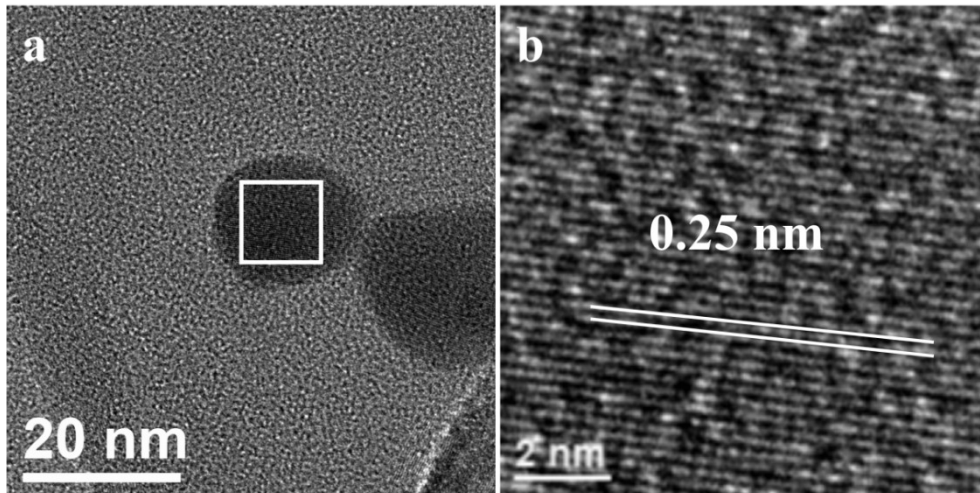


Fig.S8 HRTEM image of AgCu-T/CN with the lattice fringe of 0.25 nm assigned to Ag⁰, similar to AgCu/CN.

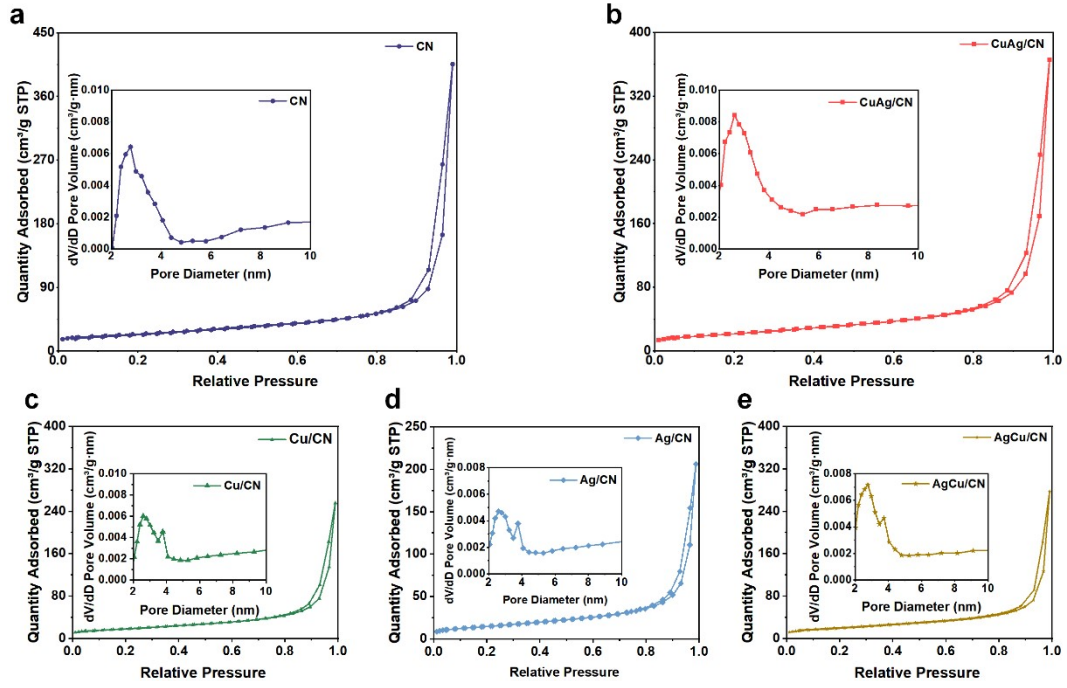


Fig.S9 Nitrogen adsorption and desorption isotherms of (a) CN, (b) CuAg/CN, (c) Cu/CN, (d) Ag/CN and (e) AgCu/CN (insert pore-size distribution curves).

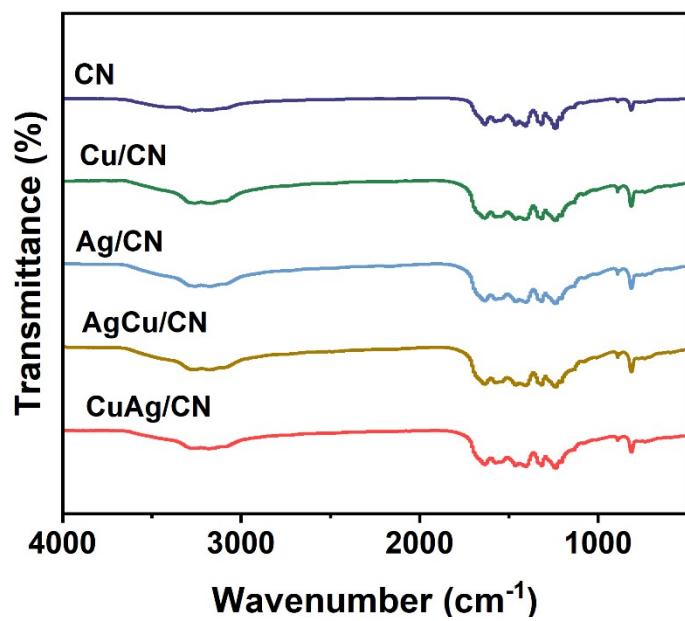


Fig. S10 FTIR spectra of CN, Cu/CN, Ag/CN, AgCu /CN and CuAg /CN.

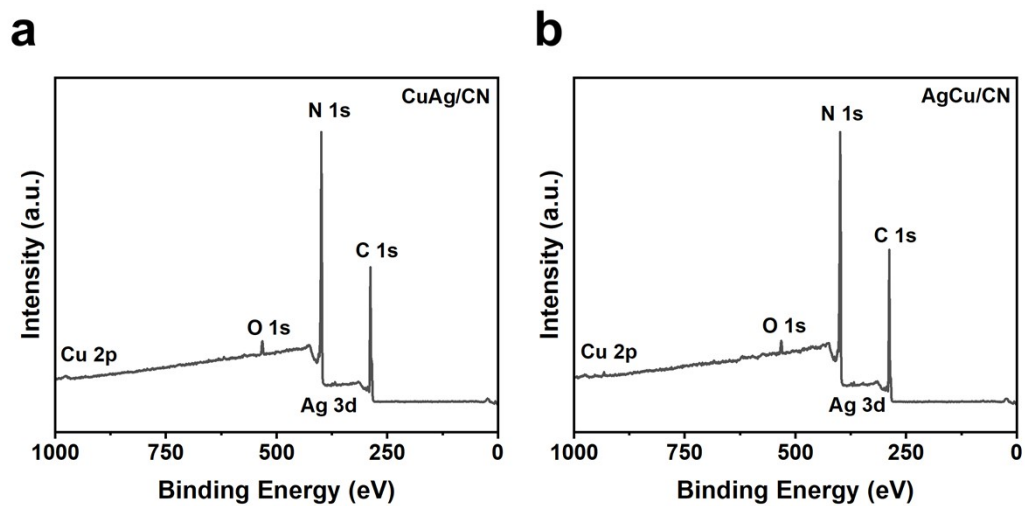


Fig. S11 XPS survey spectra of (a) CuAg/CN and (b) AgCu/CN.

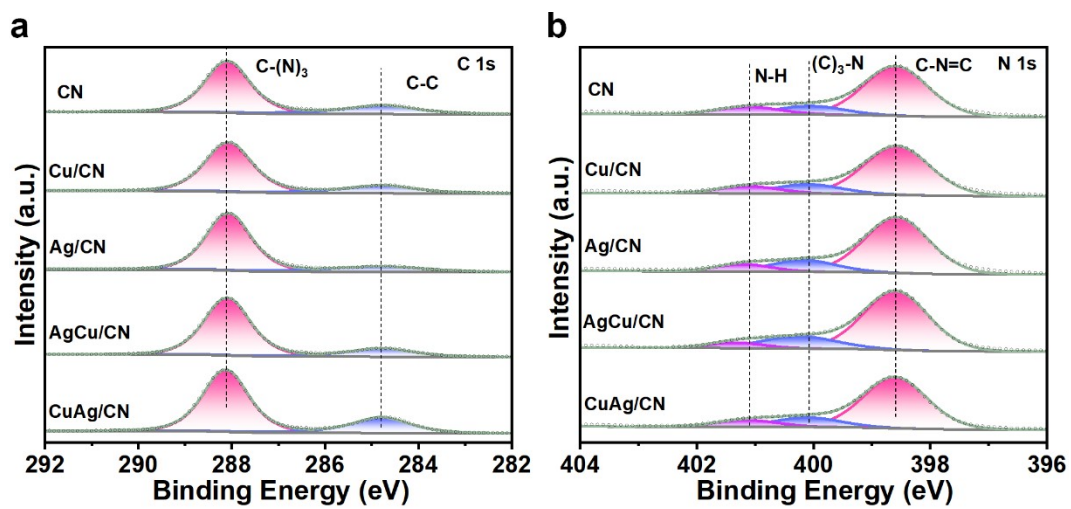


Figure S12. (a) C 1s and (b) N 1s XPS spectra of CN, Cu/CN, Ag/CN, AgCu/CN and CuAg/CN.

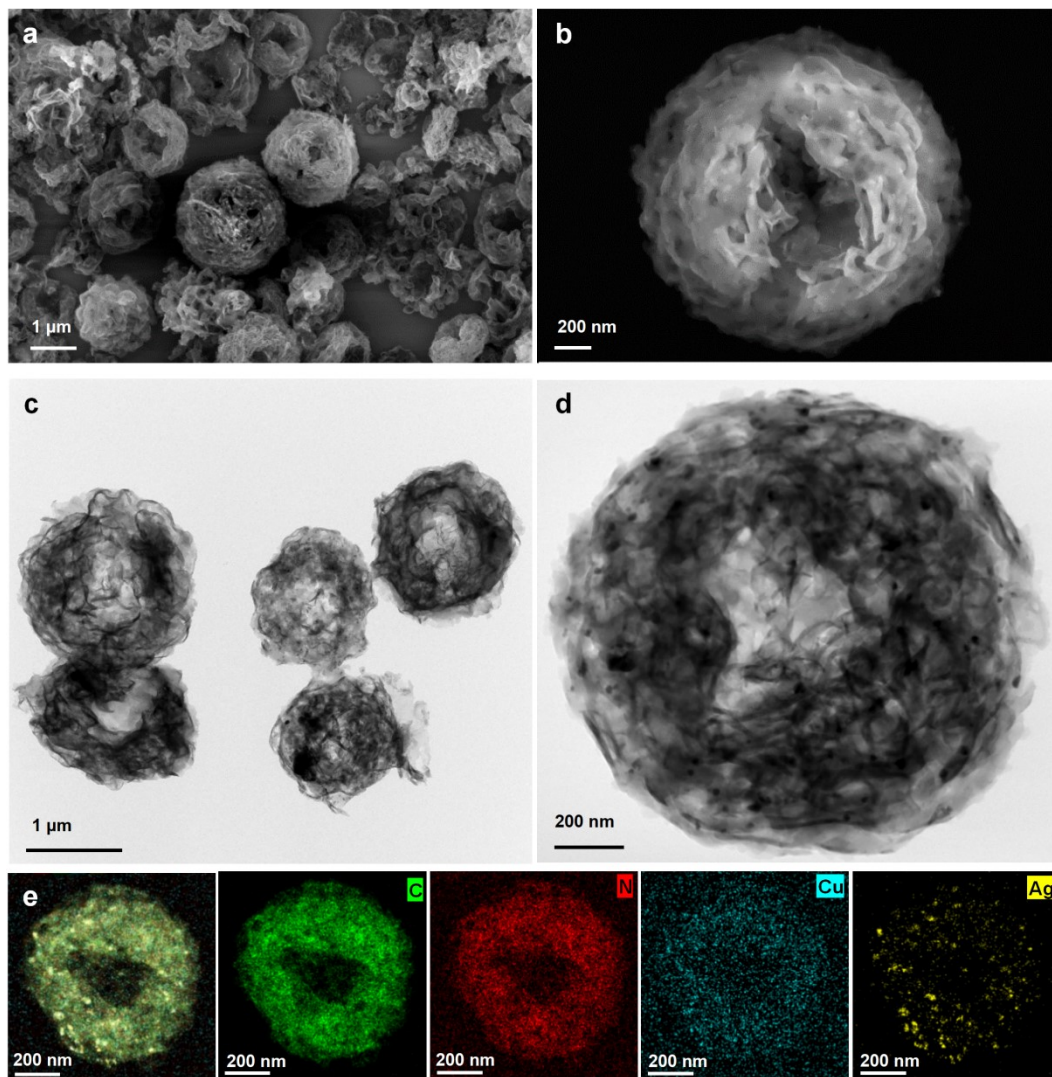


Fig.S13 (a-b) SEM image, (c-d) HRTEM image, (e) EDS elemental mapping of CuAg/CN after the cycling test.

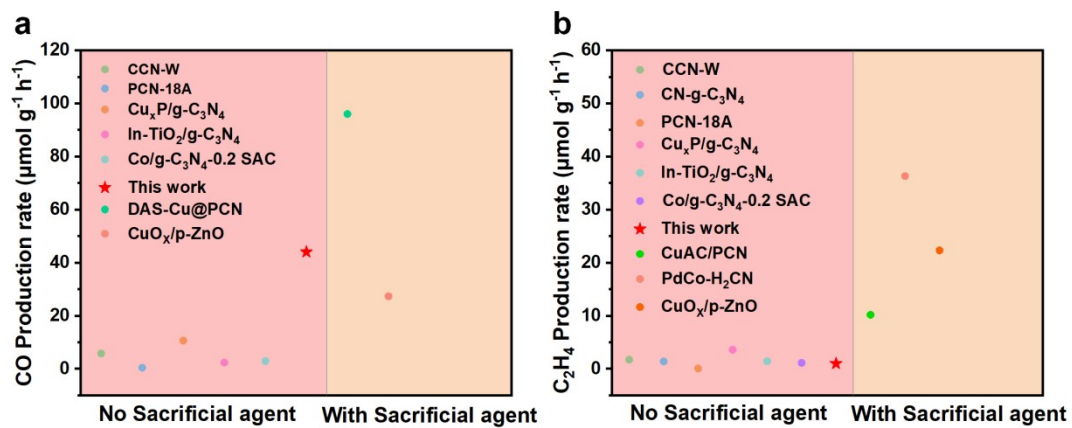


Fig.S14 Comparison of (a) CO, (b) C_2H_4 production rates of CuAg/CN reported in this work with other recently reported related photocatalysts without sacrificial agent or with sacrificial agent, respectively.

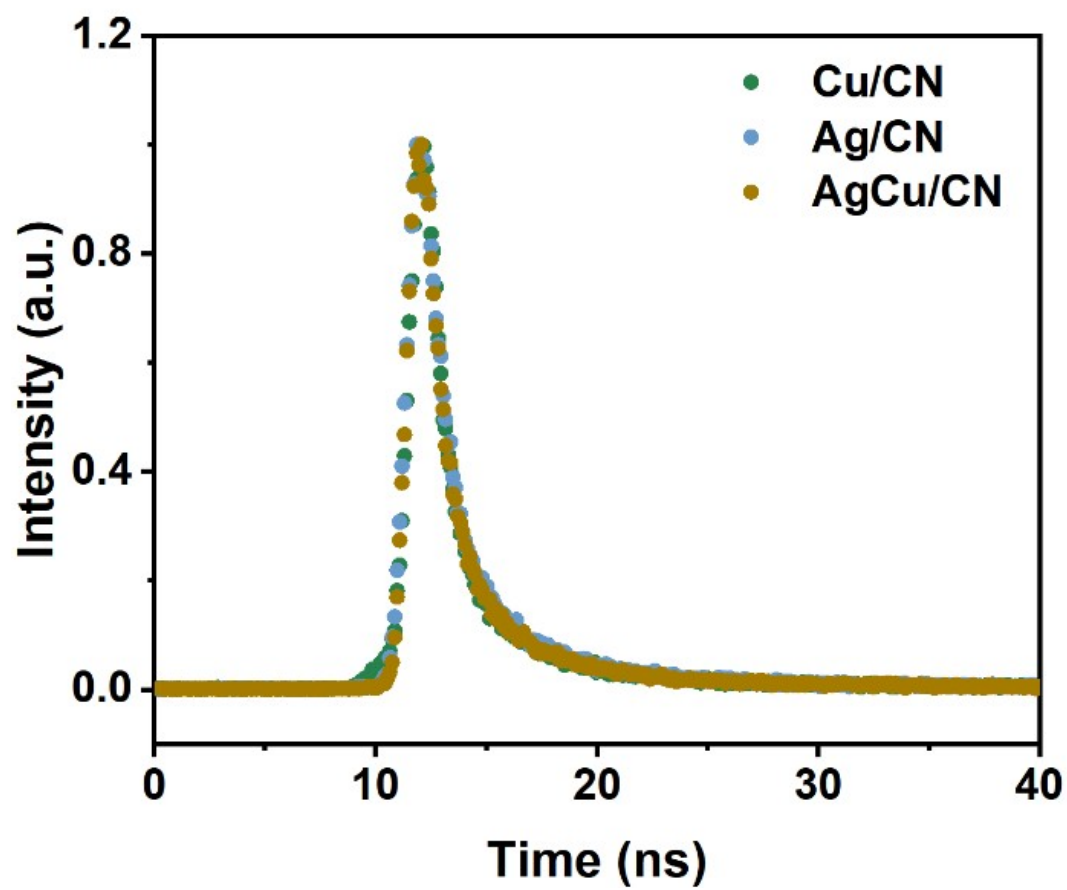


Fig.S15 Time-resolved PL spectra of CuCN,Ag/CN and AgCu/CN.

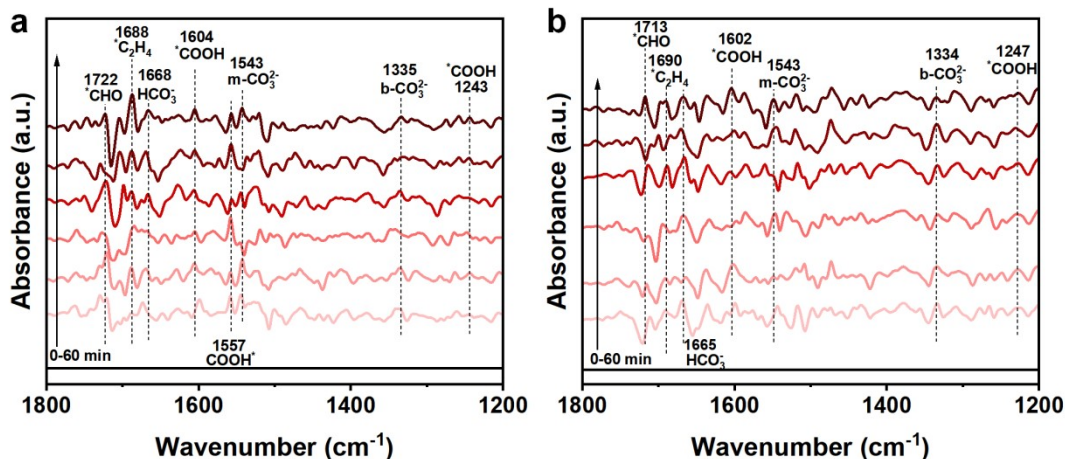


Fig.S16 In-situ DRIFTS spectroscopy of (a) CuAg/CN and (b) AgCu/CN at different irradiation time.

CuAg/CN: The absorption peaks b-CO_3^{2-} (1335 cm^{-1}), m-CO_3^{2-} (1543 cm^{-1}) and HCO_3^- (1668 cm^{-1}) were attributed to the carbonate and bicarbonate species from the dissolution of CO_2 into H_2O . The peaks at 1243 cm^{-1} and 1604 cm^{-1} were attributed to the $^*\text{COOH}$ group¹. The peaks at 1722 cm^{-1} was attributed to the $^*\text{CHO}$ group². The peaks at 1688 cm^{-1} were attributed to the $^*\text{C}_2\text{H}_4$ group³.

AgCu/CN: The absorption peaks b-CO_3^{2-} (1334 cm^{-1}), m-CO_3^{2-} (1543 cm^{-1}) and HCO_3^- (1665 cm^{-1}) were attributed to the carbonate and bicarbonate species from the dissolution of CO_2 into H_2O ⁴. The peaks at 1247 cm^{-1} and 1602 cm^{-1} were attributed to the $^*\text{COOH}$ group¹. The peaks at 1713 cm^{-1} was attributed to the $^*\text{CHO}$ group². The peaks at 1690 cm^{-1} were attributed to the $^*\text{C}_2\text{H}_4$ group³.

Supplementary Tables

Tab.S1 BET surface areas of samples

Sample	BET Surface Area (m ² /g)
CN	85.3205
Cu/CN	65.5597
Ag/CN	53.4777
AgCu/CN	69.0635
CuAg/CN	78.3660

Tab.S2 Comparison of photocatalytic activity of different samples in recently studies.

Photocatalyst	Light wavelength (nm)	Sacrificial agent	Reduction products		Rate of production ($\mu\text{mol}\cdot\text{g}^{-1}\cdot\text{h}^{-1}$)		Product selectivity		Ref
This work	300 W Xe lamp	H ₂ O	CO	C ₂ H ₄	44.0	2.4	99.5%	0.5%	
Co/g-C ₃ N ₄ -0.2 SAC	300 W Xe lamp	H ₂ O	CO	C ₂ H ₄	2.90	1.10	10.5%	0.11%	5
CCN-W	300 W Xe lamp	H ₂ O	CO	C ₂ H ₄	5.75	1.71	48.3%	14.4%	6
CN-g-C ₃ N ₄	300 W Xe lamp	H ₂ O	CH ₄	C ₂ H ₄	5.86	1.38	81.1%	19.1%	7
PCN-18A	(>400 nm) 300 W Xe lamp	H ₂ O	CO	C ₂ H ₄	0.40	0.05	82.5%	9.8%	8
Cu _x P/g-C ₃ N ₄	320-780 nm 300 W Xe lamp	H ₂ O	CO	C ₂ H ₄	10.59	3.58	73.0%	24.7%	9
PdCo-H ₂ CN	320-780 nm 300 W Xe lamp	TEOA		C ₂ H ₄		36.3			10
In-TiO ₂ /g-C ₃ N ₄	350-780 nm UV 365 nm	none	CO	C ₂ H ₄	2.32	1.41	21.0%	12.8%	11
DAS-Cu@PCN	300 W Xe lamp	TEOA	CO	C ₂ H ₆	96	118.7			12
CuAC/PCN	300 W Xe lamp	TEOA	CH ₄	C ₂ H ₄	8.95	10.17	46.8%	53.2%	13
CuO _x /p-ZnO	300 W Xe lamp 320-780nm	TEA	CO	C ₂ H ₄	27.30	22.30	40.4%	33%	14

Supplemental References

1. L. Chen, X. Yang, Z. He, J. Zheng, M. Zhu, Z. Zeng, H. Li, Y. Liu and S. Yang, *Adv. Funct. Mater.*, 2025, 35, 2500818.
2. Y. Yu, X. a. Dong, P. Chen, Q. Geng, H. Wang, J. Li, Y. Zhou and F. Dong, *ACS Nano*, 2021, 15, 14453–14464.
3. Y. Wu, Q. Chen, J. Zhu, K. Zheng, M. Wu, M. Fan, W. Yan, J. Hu, J. Zhu, Y. Pan, X. Jiao, Y. Sun and Y. Xie, *Angew. Chem., Int. Ed.*, 2023, 62, e202301075.
4. S. Hu, P. Qiao, X. Yi, Y. Lei, H. Hu, J. Ye and D. Wang, *Angew. Chem., Int. Ed.*, 2023, 62, e202304585.
5. M. Ma, Z. Huang, D. E. Doronkin, W. Fa, Z. Rao, Y. Zou, R. Wang, Y. Zhong, Y. Cao, R. Zhang and Y. Zhou, *Appl. Catal. B*, 2022, 300, 120695.
6. Y. Liang, X. Wu, X. Liu, C. Li and S. Liu, *Appl. Catal. B*, 2022, 304, 120978.
7. Q. Gao, W. Qi, Y. Li, Y. Wei, Y. Wu, X. Liang, Y. Zhang, Y. Hu, P. Wang, Q. Chen, X. Chen and Y. Zhu, *Small*, 2024, 20, 2404822.
8. Z. Fang, Q. Wang, X. Zhao, Y. Li, W. Zhang and D. Zhang, *J. Environ. Chem. Eng.*, 2023, 11, 109478.
9. D. Wen, N. Wang, J. Peng, T. Majima and J. Jiang, *Chin. J. Catal.*, 2025, 69, 58–74.
10. C. Huang, X. Yu, G. Lv, Y. Hu and L. Liao, *J. Mater. Chem. A*, 2025, 13, 34948–34954.
11. J. Park, H. Liu, G. Piao, U. Kang, H. W. Jeong, C. Janáky and H. Park, *Chem. Eng. J.*, 2022, 437, 135388.
12. X. Cao, C.-Y. Liu, Y. Dong, T. Yang, X. Chen and Y. Zhu, *Catal. Sci. Technol.*, 2024, 14, 2003–2011.
13. W. Xie, K. Li, X. H. Liu, X. Zhang and H. Huang, *Adv. Mater.*, 2022, 35, 2208132.
14. W. Wang, C. Deng, S. Xie, Y. Li, W. Zhang, H. Sheng, C. Chen and J. Zhao, *J. Am. Chem. Soc.*, 2021, 143, 2984–2993.